AD-A066 547 GEORGIA INST OF TECH ATLANTA FRACTURE AND FATIGUE RE--ETC F/G 11/6
THE EFFECT OF ION PLATING AND ION IMPLANTATION ON THE CYCLIC RE--ETC(U)
MAR 79 S SPOONER, H SOLNICK-LEGG, E A STARKE N00014-78-C-0270

UNCLASSIFIED NL

END
DATE FILMED
5-79
DDC

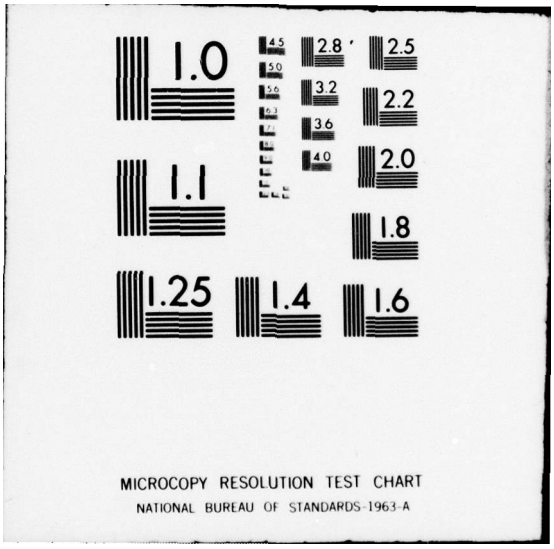
1.0
1.1
1.25
1.4
1.6
1.8
2.0
2.2
2.5
2.8
3.2
3.6
4.0
4.5
5.0
5.6
6.3
MICROCOPY RESOLUTION TEST CHART
NATIONAL BUREAU OF STANDARDS-1963-A

SECURITY CLASSIFICATION (When Data Entered)

036-128

REPORT DOCUMENTATION PAGE

READ INSTRUCTIONS BEFORE COMPLETING FORM

1. REPORT NUMBER: Technical Report No. 1
2. GOVT ACCESSION NO.
3. RECIPIENT'S CATALOG NUMBER
4. TITLE (and Subtitle): The Effect of Ion Plating and Ion Implantation on the Cyclic Response and Fatigue Crack Initiation of Metals and Alloys.
5. TYPE OF REPORT & PERIOD COVERED: rept no. 1 — Technical, 1 Mar 78 - 28 Feb 79
6. PERFORMING ORG. REPORT NUMBER
7. AUTHOR(s): S. Spooner, H. Solnick-Legg, E. A. Starke, Jr.
8. CONTRACT OR GRANT NUMBER(s): N00014-78-C-0270
9. PERFORMING ORGANIZATION NAME AND ADDRESS: Fracture and Fatigue Research Laboratory, Georgia Institute of Technology, Atlanta, Georgia 30332
10. PROGRAM ELEMENT, PROJECT, TASK AREA & WORK UNIT NUMBERS: 12 / 29p.
11. CONTROLLING OFFICE NAME AND ADDRESS: Office of Naval Research, 800 N. Quincy Street, Arlington, Virginia
12. REPORT DATE: March 1979
13. NUMBER OF PAGES: 30
14. MONITORING AGENCY NAME & ADDRESS (if different from Controlling Office)
15. SECURITY CLASS. (of this report): Unclassified
15a. DECLASSIFICATION/DOWNGRADING SCHEDULE

LEVEL II

16. DISTRIBUTION STATEMENT (of this Report)

Approved for Public Release; Distribution Unlimited

17. DISTRIBUTION STATEMENT (of the abstract entered in Block 20, if different from Report)

18. SUPPLEMENTARY NOTES

19. KEY WORDS (Continue on reverse side if necessary and identify by block number)

Ion Implantation
Ion Plating
Fatigue Crack Initiation
Copper

20. ABSTRACT (Continue on reverse side if necessary and identify by block number)

X-ray diffuse scattering and transmission electron microscopy have been used to study the defect state of copper implanted with aluminum and argon ions. Electron microscopy studies of argon implanted thin foils reveals vacancy loops in the size range of 70Å to 350Å diameter for a dose of 2×10^{15} ions cm^{-2} at 100 kev. X-ray diffuse scattering measured around the 222 Bragg reflection reveals a combination of microalloying and dislocation loop effects from implantation of aluminum ions to a dose of 2×10^{16} ions cm^{-2} at 100 kev. Loop densities on the order of 10^{17} cm^{-2} and an average loop size of 25Å was

2 x 10 to the 15th power ions/sq. cm

10 to the 17th power/sq. cm.

2 x 10 to the 16th power ions/sq cm

DD FORM 1 JAN 73 1473 EDITION OF 1 NOV 65 IS OBSOLETE

SECURITY CLASSIFICATION OF THIS PAGE (When Data Entered)

estimated from the x-ray data. The aluminum ion damage is largely unchanged upon annealing for 30 minutes at 500° and 600°C. Alloying appears to stablize the surface radiation damage relative to damage produced in self-ion bombardments. The possible effectiveness of implanted layers in affecting fatigue crack initiation is being assessed.

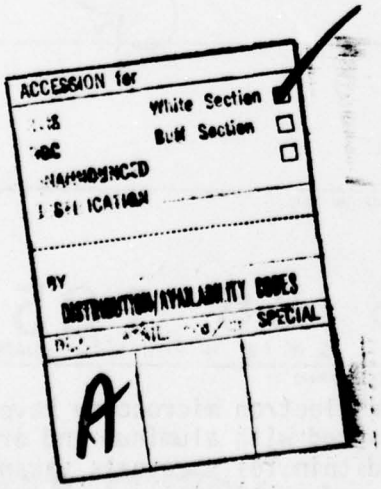

The Effect of Ion Plating and Ion Implantation on the Cyclic Response and Fatigue Crack Initiation of Metals and Alloys

Technical Report 1
For the Period
1 March 1978 - 28 February 1979

March 1979

by

S. Spooner, H. Solnick-Legg and E. A. Starke, Jr.

Prepared for the Office of Naval Research
Department of the Navy, under Contract
N00014-78-C-0270

Approved for public release; distribution unlimited

Fracture and Fatigue Research Laboratory
Georgia Institute of Technology
Atlanta, Georgia 30332

TABLE OF CONTENTS

LIST OF FIGURES

ABSTRACT

X-ray diffuse scattering and transmission electron microscopy have been used to study the defect state of copper implanted with aluminum and argon ions. Electron microscopy studies of argon implanted thin foils reveals vacancy loops in the size range of 70Å to 350Å diameter for a dose of $2X10^{15}$ ions cm^{-2} at 100 kev. X-ray diffuse scattering measured around the 222 Bragg reflection reveals a combination of microalloying and dislocation loop effects from implantation of aluminum ions to a dose of $2X10^{16}$ ions cm^{-2} at 100 kev. Loop densities on the order of 10^{17} cm^{-3} and an average loop size of 25Å was estimated from the x-ray data. The aluminum ion damage is largely unchanged upon annealing for 30 minutes at 500° and 600°C. Alloying appears to stablize the surface radiation damage relative to damage produced in self-ion bombardments. The possible effectiveness of implanted layers in affecting fatigue crack initiation is being assessed.

I. BACKGROUND

Modern design philosophies, which are greatly affected by economical and safety factors, require the use of materials having an optimum combination of properties, e.g., fabricability, strength, facture toughness, corrosion and fatigue resistance. It is difficult to obtain alloys, either by design or through empirical development, having the required combination since the alloy chemistry and microstructure desired for certain properties may be detrimental to others. For example, aluminum alloys which show the highest static strength are inherently susceptable to stress corrosion cracking[1] and have poor fatigue resistance.[2] However, for most alloy systems corrosion and fatigue behavior are greatly affected by the surface condition and surface related phenomena, and may be improved (or controlled) by altering the state of the surface without adversely changing bulk properties, e.g., fracture toughness, yield strength, and ductility.

Metallic coatings have been widely used in industry for controlling corrosion and errosion. The principle of this technique is to separate the metal being protected from the unfavorable surroundings. An improvement arises from the inertness of the coating material with the environment. Many coating techniques are now available, and include hot dipping, metal spraying, electroplating, vacuum deposition, and diffusion coatings. These methods can be divided into two general groups: those which create an abrupt interface with a composition discontinuity between the coating surface and the substrate, and those which create a composition varation at the interface. Most of these coating methods produce an undesired contaminated interface which may prove detrimental when the sample is under static or dynamic loading. For example, during electroplating there may be a simultaneous reaction (e.g., water is

often reduced to form hydrogen) which may have a considerable influence on the mechanical properties. In addition, electroplated layers can have a wide range of compressive and tensile stresses depending upon the plating parameters, and may contain networks of microcracks with varying depths and spacing.[3] The more recent ion plating and ion implantation methods produce a clean, strongly-adherent interface between the coating material and substrate. The compositional variation at the interface can be controlled by controlling the energy of the ions.

Although it is generally agreed that fatigue cracks originate and propagate from a free surface and that the surface condition has a considerable effect on fatigue life, research on the influence of surface films on fatigue behavior has been lacking. The fatigue process may be divided into two general areas: crack initiation and crack propagation. Improvements in fatigue life can be obtained by increasing the time to crack initiation or reducing crack growth rates, or both. However, crack initiation is more affected by the surface condition than is crack propagation, and consequently the possibility exists for improving the fatigue performance by altering the state of the surface, without greatly changing bulk properties. The present ONR program is concerned with the effects of various ion-plated and ion implanted surfaces, and their microstructure, on the CSSR and fatigue crack initiation of a copper substrate. To meet the program objectives we have selected surface film-substrate combinations designed to separate the various parameters which control near surface deformation and associated crack initiation.

The influence of ion-plated surface films and/or implanted surfaces on fatigue crack initiation depends on such parameters as: crystal structure,

stacking fault energy, composition, and mechanical properties of the surface region and the substrate; the degree of misfit and cleanliness at the interface, the residual stresses in the film and substrate (due to radiation damage and the accommodation dislocation network) and the adhesion of the film. The complex interrelationships between these parameters, as well as which ones dominate for a given system, are presently not well understood. Consequently, the behavior of such composites is now largely unpredictable. Our effort during the first year of this program has been mainly concerned with studying the surface structure of copper single crystals implanted with aluminum and argon ions. Studies of fatigue crack initiation in similarily implanted crystals is now underway. Concurrently, we are studying the effect of ion plating on the low cycle fatigue behavior of polycrystalline copper. However, this report is concerned only with our preliminary results on the characterization of ion implanted copper single crystals.

II. INTRODUCTION

Although ion implantation effects are confined to very thin layers, several kinds of property improvements are effected by this method of surface treatment. Mechanical wear resistance dramatically increases so that wire drawing die life is quantitatively extended in the case of ion implantation of steel dies.[4] Ion plating which combines aspects of vaper deposition with aspects of low energy implantation at the substrate/plating interface has been demonstrated to modify the fatigue crack initiation resistance in copper single crystals.[5] Vapor deposition alone can change mechanical properties of copper[6] but the additional effects of ion damage on mechanical properties remains unexplored. There are many fundamental studies of the structure of ion implantation damage

related neutron damage simulation[7] and semi-conductor device physics.[8] The structure of the implanted layer can be modified in a controlled way by choice of ion, energy and dose. In approaching the possible application of implantation alloying and damage effects to fatigue crack initiation, one must answer several fundamental questions: (1) How do ion-type and implantation energy affect surface layer structure and structure stability, (2) How do the various implantation structures affect fatigue crack initiation mechanisms, and (3) which structures are helpful or detrimental to mechanical property improvements. A partial answer is given in a recent presentation on the effects of platinum ion plated titanium in which subsurface crack initiation was reported.[9]

A basic inquiry into the first question has been initiated with transmission electron microscopy and diffuse x-ray scattering studies of ion damage structure in copper. The single crystal method adopted for this investigation[10] is capable of measuring surface layer distortion and the density of dislocation loop produced by ion damage. The combination of these two methods aims at direct characterization of damage type and density and surface strain state measurement. This preliminary work describes some findings on the nature of sessile loops produced in copper by argon ion damage and the character of combined microalloy and sessile loop structure in aluminum-implanted copper. There are indications of irradiation damage stability in x-ray difuse scattering from annealed microalloys.

III. EXPERIMENTAL

Aluminum ion implantation of copper was selected on the basis of a favorable substitutional solubility combined with an easily measured alloy lattice parameter change. In addition, the relatively light ion can penetrate deeply into the copper substrate.

Copper single crystal surfaces parallel to (111) were prepared in bulk material or thin foil TEM discs for ion implantation. TEM discs were mechanically cut, electropolished and then teepanned into 3 mm discs. These discs were etched chemically and then finally thinned with a TENUPOL double-jet electro polisher until perforation. These foils were examined in the JEOL 100C electron microscope for selection of low dislocation density samples for later implantation.

Highly perfect crystals were selected for x-ray studies in order to ensure that pre-existing dislocation effects would not interfere with ion-implantation effects. Bulk copper crystals were provided by F. W. Young of Oak Ridge National Laboratory. These crystals were grown by Bridgeman technique and then annealed for two weeks at a few degrees below the melting point. The crystals were radiation hardened with neutrons before final cutting to orientation. Chemical cutting techniques were used to shape the crystal. The dislocation densities measured after final sample preparation, but prior to ion implanation, was less than 10^3 cm^{-2}.

The TEM discs and bulk crystals were oriented with (111) surface normals 6° from the incident beam direction to prevent channeling (even through [111] channeling in copper is very unfavorable). The Accelerators, Inc. 200 kev Ion Implanter was used to irradiate the crystal surfaces at 25°C. Temperature rises in these samples have not been measured. However, bulk samples are not expected to see more than a few degrees centigrade rise since the crystal substrate is a good heat sink. The TEM foils are mounted in mechanical contact with a good heat sink, but since the degree of thermal contact is unknown a temperature rise of several 10's of degrees C is possible at a high dose rate. Argon dose rates

at 100 kev were $3X10^{12}$ ions cm^{-2} sec^{-1}. The total dose was $2X10^{15}$ ions cm^{-2}. Bulk crystals were implanted with three doeses for the purpose of providing an approximately level implanted ion concentration from the surface to the maximum depth range at 200 kev. The implantation area of 3 mm diameter was placed to one side of the surface in order that x-ray diffraction measurement could be made on both implanted and unimplanted areas on the same crystal surface. Dose rates were as follows: $19.7X10^{13}$ ions cm^{-2} sec^{-1} at 200 kev, $9.9X10^{12}$ ions cm^{-2} sec^{-1} at 100 kev and $2.4X10^{11}$ ions cm^{-2} sec^{-1} at 50 kev. The does were $2X10^{16}$ ions cm^{-2}, $4X10^{15}$ ions cm^{-2} and $5.5X10^{15}$ ions cm^{-2} respectively. An aluminum concentration of 2 atomic percent is calculated to have been generated to a thickness of 1000 Å. The ion implanter beam line vacuum was $2X10^{-5}$ Torr during implantations. The ion implantation machine is now being modified to provide implant concentration profile determinations. In these studies theoretical estimates of implant distribution were used. Annealing studies were carried out on the bulk crystals at 500°C, 600°C, and 900°C in a vacuum of $\sim 10^{-6}$ Torr for 30 minutes.

The x-ray measurements were carried out with apparatus at the Oak Ridge National Laboratory. The diffuse scattering was measured in a two-axis x-ray spectrometer with Cu Kα radiation monochromated with the 333 reflection of a silicon crystal. The x-rays impinge on the (111) surface at approximately 45° and radiation scattered in the vicinity of the 222 reflection is intercepted by an open detector set at 90° from the incident beam. The scattering geometry is shown in Figure 1. The scattered intensity is measured as a function of the copper crystal rocking angle, $\Delta\Theta$, after the crystal has been carefully oriented to give a maximum peak reflectivity. The measured intensities are scaled to

the incident beam intensity of an approximately 2 mm diameter beam measured by the open detector positioned to intercept the beam through a calibrated filter.

TEM investigations concentrated on the observation of the relatively large loops found in the argon implanted foils. The theoretical argon ion distribution is peaked at 350 Å for 100 kev. Therefore it is estimated that a significant fraction of the damage will be deposited in the TEM foil. Sessile loops were identified by observing the variation of loop contrast with changing diffraction vector used for image contrast. The loop-type was identified by assuming a Burgers vector b = a/3 <111> and the collapse planes of {111}. Use of single crystals greatly facilitates the orientation analyses.

IV. RESULTS

The diffuse scattering measurements made on an aluminum implanted copper crystal are shown in Figure 2. The logarithm of the normalized scattering intensities of the implanted and un-implanted crystals are plotted as a function of the rocking angle $\Delta\Theta$ relative to the substrate Bragg peak position. An intensity increase arising from implantation is seen on both low and high angle sides of the Bragg peak. A general intensity increase is larger at low angles and no obvious side peak is seen. The qualitative character of the intensity is consistent with scattering from a Cu(Al) alloy whose lattice parameter is larger than that of the pure copper substrate. As will be discussed below, calcuated alloy layer scattering effects predict scattering in the form of a low angle peak with $I^S/I_o \sim 0.01$ with much smaller contribution, at high angles (I^S = scattered intensity and I_o is incident power). Therefore, additional diffuse scattering is present in the form of dislocation loop scattering. Such scattering arises from damage within the microalloy region. Thus, this diffuse

scattering must be peaked at an angle which is displaced toward the low-angle side from the substrate Bragg peak position. Presently no quantitative calculation of combined microalloying and damage effect scattering can be made. But recent self-ion damage results on nickel[11] provides some guidance on effects to be expected from loops alone. For the nickel study in which $5X10^{13}$ ions cm^{-2} were implanted at 4 Mev, points defects produced[12] were a factor of 20 less than that of the aluminum implantation of this study. The scattering intensity (I^S/I_o) seen in the nickel study was on the order of 10^{-3} in the angular range of interest. If the nickel scattering intensities were scaled up in proportion to the number of point defects produced then the scaled intensity would be in the range of scattering observed in our experiments. Thus, loop scattering and microalloying effects are comparable in their contribution to the integral diffuse scattering effect.

The results from integral diffuse scattering measurements for as-implanted and 500°C (T/T_M = 0.56) for 30 minutes annealed material is shown in Figure 3. This curve shows the difference between intensities taken from the implanted and unimplanted areas. Figure 4 shows similar data for a second crystal which was annealed at 600°C (T/T_M = 0.64) for 30 minutes. (The data in this figure may be compromised by the surface roughness of the sample although the trend shown in the annealing effects is at least qualitatively correct). The important finding is that the loop scattering (which is indicated most cleanly on the high angle side of the rocking curve) does not significantly change with annealing. This result should be compared with the observation that a 25% decrease in scattering from nickel self-ion implanted crystals was observed upon annealing at 450°C (T/T_M = 0.42) for one hour. Finally, although not shown, it

was observed that a 900°C (T/T_M = 0.86) annealled for 30 minutes entirely removed scattering effects from the crystal which was initially annealed at 500°C.

TEM micrographs of argon implanted foils are shown in Figure 5. Dislocation loops are visible near bend contours which contribute to the contrast. At least one-third of the larger loops present will not be visible due to image contrast geometry and no analysis for "black dot" loops was attempted. Several of the more easily seen loops (up to 350 Å diameter) were analyzed as vacancy type. This was determined on the basis of an "inside-outside" contrast variation with a change from one known diffraction vector to another. An estimate of the loop density of the larger loops was done assuming that one-third of the dislocations were observed in the damage thickness of 350 Å. The calculation gave $4X10^{10}$ loops cm^{-3}. If an average loop size of 100 Å diameter is assumed, then the number of point defects residing in loops is $2X10^{14}$ cm^{-3} which is lower than the density of Frenkel pairs which one calculates for the argon implantation dose. A calculation of dislocation density gives 10^6 cm^{-2} which is a density found in moderately annealed material.

V. DISCUSSION

TEM is essential for the determination of the dislocation loop type through contrast analysis. This kind of determination is not feasible with the present diffuse scattering method and would be difficult under the best of circumstances in the case of mixed vacancy and interstitial loop population. The observation of large loops in the estimated density found in argon implanted copper is consistent with the possibility of thin foil heating during implantation. The interstitials have enough mobility to leave the foil surfaces which are but a few tens of atomic diameters away from an average interstitial. A small amount of temperature rise may allow vacancy migration to go to larger loops which is

energetically favorable. In summary, one can expect to see elimination of interstitials and their loops and the growth of vacancy loops. Such a plausibility is born out in the TEM results which indicate vacancy loops at a density corresponding to moderately annealed material. As these studies progress, TEM methods employing back thinning will be used increasingly for the purpose of complementary TEM and x-ray studies of a identically implanted copper.

The x-ray diffuse scattering measurements can be compared against microalloy scattering estimates and loop scattering measurements made on self-ion implanted nickel.[11] Microalloy effects were estimated on the basis of a dynamical diffraction calculation originally done for elastically bent crystals.[13] Larson et al[14] have applied this approach to boron implanted silicon. Two coupled differential equations are written for the derivatives of the real and imaginary components of the scattering amplitude with respect to distance normal to the surface. These equations include a term describing the lattice strain as a function of depth due to a distribution of implanted solute. The lattice strain was taken to arise from the aluminum alloying lattice parameter change. The aluminum distribution was described by an approximation to the theoretical implantation profile. Numerical integration of the coupled differential equations was done with a differential equation solver available from the computer center library. The calculation sequence was as follows. At a given rocking angle, the real and imaginary components of the scattering amplitude was calculated for a perfect crystal[15,16]. These components were used as initial values for the integration into the crystal to a depth below the implanted ions. The real and imaginary components at this depth were then used as initial values for integration back to the free surface but with the intervening material now modified to include lattice distortions. The resulting amplitude at the free

surface gave the reflectivity of the crystal at the particular rocking. A sequence of these calculations gives the rocking curve shown in Figure 6. The small peak appearing at low angle has an associated d-spacing corresponding to the assumed 1 atomic percent alloy. The peak reflectivity of approximately 1% is of the right magnitude to correspond to observed scattering intensity. The model for the lattice strain used in the calculation does not take lattice relaxation at the interface between implanted and unimplanted material into account. There is expected to be a gradient in lattice parameter which would tend to broaden the scattering peak and therefore the scattering is distributed over wider angles at a lower intensity. When quantitative measurements of implantation profiles can be made with the implantation device on identically prepared material, further refinements of the above calculation will be attempted.

The diffuse scattering (I^S/I_o) from dislocation loops seen in self-ion implanted nickel is in the range of 10^{-3} over a wide angular range. The scattering of small rocking angles--Huang scattering--arises from the long-range loop strain fields and is characterized by a proportionality to $-\ln(\Delta\Theta)$. A larger angle scattering proportional to $(\Delta\Theta)^{-2}$ arises from short-range strain fields. In the aluminum implantation of copper, dislocation loops are created within the microalloy region. Thus, loop scattering build-up centers at the Bragg peak angle of the microalloy. This explains why there is a broad asymmetry of scattering in Figures 3, 4 and 5. It was necessary to estimate the Bragg peak center from the lattice expansion expected in a 2 atomic percent alloy with the result that $\Delta\Theta_{Bragg} = 3.9$ min. The diffuse scattering was plotted in Figure 7 where $\Delta\Theta$ was measured relative to the displaced microalloy Bragg peak. The average scattering calculated from

$$\bar{I} = (I^S(+)/I_o + I^S(-)/I_o)/2$$

was extrapolated to zero on the $\bar{I}$ vs $\ln(\Delta\Theta)$ curve to obtain $\Delta\Theta^*$. This value can then be used to obtain an average loop diameter from the relation[10] where

$$R_o = (e^{\frac{1}{2}} q_o^*)$$

where $q_o^* = h\,\Delta\Theta^* \cos\Theta_B$ and $h = 2\pi/d_{222}$. The average loop radius obtained in this calculation is 25 Å, but it must be kept in mind that loop radius size distributions have been found to be a strongly decreasing exponential[11] in form so that the average loop radius must be interpreted carefully.

An advantage in this scattering technique is that the measured intensity can be calculated with no arbitrary constants. Thus, parameters used for describing the loop size distribution can be obtained from an analysis of the measurements. For example, the Huang scattering occurring at small rocking angles can be calculated for a single loop size, R, having a specified loop density, C_r, which comes from the above described intensity extrapolation method. Hence

$$I^3(q_o)/I_o = K\,C_L R^4 \ln (q_o^*/q_o)$$

where $q_o = hq_o \cos\Theta_B$ and K is a calculable constant which depends on known physical constants of the material. More physical models of loop size distribution such as the exponential form mentioned above ($C_L(R)\,C^{-R/R_o}$) can be used in similar equations to make quantitative comparisons with scattering data. For the time being it will be simpler to make qualitative comparisons of aluminum implant scattering with nickel self-ion implant scattering[11].

A simple Kinchen-Pease model for Frenkel defect (vacancy-interstial) production can be used to scale the expected scattering effects.( ) The number of defects per ion is given by

$$\nu(E_R) = \frac{0.8\ E_d}{2\ E_D^{avg}}$$

where E_R is the recoil energy, E_d is the recoil energy corrected for electronic energy loss, and E_D^{avg} is the average displacement energy. The ratio of defects produced in copper by 200 kev aluminum ions and in nickel by 4 Mev nickel ions is approximately 20 after dose differences are taken into account. A comparison of Huang scattering for the two cases is shown in Figure 8. Only a factor of 7 is seen which can be justified on several grounds. First, displacement cascades are smaller and distributed more deeply for aluminum in copper suggesting a tendency toward smaller loops. Second, saturation effects due to dose rate may lead to more point defect anhililation. Third, copper is at a higher homologous temperature at room temperature thus favoring point defect loss. Thus, loop scattering at low angles which favors large loops may be relatively lower in the aluminum implantation case. Nevertheless, loop densities on the order of 10^{17} cm^{-3} are estimated on the basis of densities quoted in the work on nickel. The x-ray results on as-implanted copper are satisfactorally interpreted in terms of a microalloy lattice parameter expansion and creation of a high dislocation loop density with an average loop size of 25 Å. More quantitative loop density interpretations are possible with measurements of scattering to larger rocking angles.

The annealing response of the aluminum implants shown in Figure 3 and Figure 4 points out that the dislocation loops are in a thermally stable

configuration. Both aluminum alloying and loop entanglement at high doses may account for this stability. Annealing at 500°C produces only subtle intensity changes, indicating that little or no aluminum transport has occurred to smooth out the composition gradient. Neither has there been a quantitative change in loop density or size distribution change. At 600°C, however, there has been a clear change in the asymmetry of scattering with only a 20% to 30% decrease in diffuse scattering tails. This suggests that the aluminum impurity transport is fast enough for aluminum to diffuse into the substrate. This results in a restortation of the original lattice parameter but since the loop structure remains largely intact, loop scattering persists but is now centered at the main Bragg peak position. With carefully chosen annealing treatments, it appears possible to eliminate microalloy affects and thereby a separation of the two effects becomes possible. Of more practical significance is the observation of a high thermal loop structure stability and hopefully a high mechanical stability for aluminum implantation. A comparable reduction of loop scattering was observed for one hour in nickel at 425°C with a homologous temperature of 0.42. The changes at 600°C in copper at a homologous temperature of 0.64 attest quantitatively to an appreciable stability.

The strain effects seen in aluminum implanted copper can be divided into a net strain due principally to microalloying and a fluctuating strain arising from dislocation loops. In the case studied by x-rays the net strains put the surface layer in compression as the copper lattice attempts to maintain coherency with the implanted layer. This is the desired stress condition for fatigue prevention. The loop distribution is likely to respond to this stress field although it is not obvious what response in loop density or loop-type distribution might be found. Further characterization of the surface layer will be needed.

Electron channeling is under consideration as a method for eventual use in our laboratory. Sensitive measurements of lattice strain are possible by this technique and results could corroborate x-ray diffraction trends.

As more implantation species are investigated, the relation between micro-alloying and loop stability will be explored. Detailed characterization of interstitial or substitutional implants will be needed especially in cases of highly metastable alloy combinations. To this end, consideration is being given to ion channeling for indification of lattice disruption effects.

VI. SUMMARY

The feasibility of TEM and x-ray scattering methods to characterize implantation microstructure has been demonstrated. Preliminary results indicate that substantial surface damage is induced in copper by aluminum implantation. Annealing response demonstrates that the damage state is stable. However, the observed stability is a function of the implantation ion. We are now in a position to quantitatively investigate surface strain, loop type and density of new implants. Fatigue crack initiation experiments will soon be started on implanted copper samples so that favorable microstructures can be identified.

VII. ACKNOWLEDGEMENTS

The authors would like to thank Dr. B. C. Larson and Mr. Jim Barhorst of ORNL for considerable aid in collection of the scattering data and many useful discussions. In addition, we would like to express our appreciation to Dr. Keith Legg for performing the implantations used in these investigations.

VIII. REFERENCES

1. M. O. Speidel, Met. Trans. A, 1975, Vol. 6A, p. 631.

2. M. E. Fine, Met. Trans. A., 1975, Vol. 6A, p. 625.

3. R. W. Staehle, in Surface Effects in Crystal Plasticity, R. M. Latanision and J. T. Fourie, eds., NATO Advanced Study Institute Series No. 17, Noordhoff-Leyden, 1977, p. 589.

4. G. Dearnaley and N. E. W. Hartley, Thin Solid Films, 1978, Vol. 54, p. 215.

5. E. Y. Chen and E. A. Starke, Jr., Materials Sci. Eng., 1976, Vol. 24, p. 209.

6. B. R. Livesay and E. A. Starke, Jr., Acta Met., 1973, Vol. 21, p. 247.

7. P. D. Townsend, J. C. Kelly and N. E. W. Hartley, Ion Implantation, Sputtering and Their Application, 1976, Chp. 4.

8. J. Stephen, in Ion Implantation, G. Dearnaley et al. eds, North-Holland Publ. Co., 1973, Chp. 5.

9. S. Fujishiro, "Improved High Temperature Mechanical Properties of Titanium Alloys by Pt Ion Plating," paper 9/18 in Int. Conf. Metallurgical Coatings, April 3-7, 1978, San Francisco.

10. B. C. Larson, J. Appl. Cryst., 1975, Vol. 8, p. 150.

11. J. Naryan and B. C. Larson, J. Appl. Phys., 1977, Vol. 48, p. 4536.

12. K. L. Merkle, in Radiation Damage in Metals, N. L. Peterson and S. D. Harkness eds., ASM, 1976, pp. 58-88.

13. B. Klar and F. Rustichelli, Nvovo Cimento, Vol. 13B, 1973, p. 249.

14. B. C. Larson, C. W. White and B. R. Appleton, Appl. Phys. Lett., 1978, Vol. 32, p. 801.

15. B. E. Warren, X-Ray Diffraction, Addison-Wesley, 1969, Chp. 14.

16. W. H. Zachariasen, Theory of X-Ray Diffraction in Crystals, Dover, 1967.

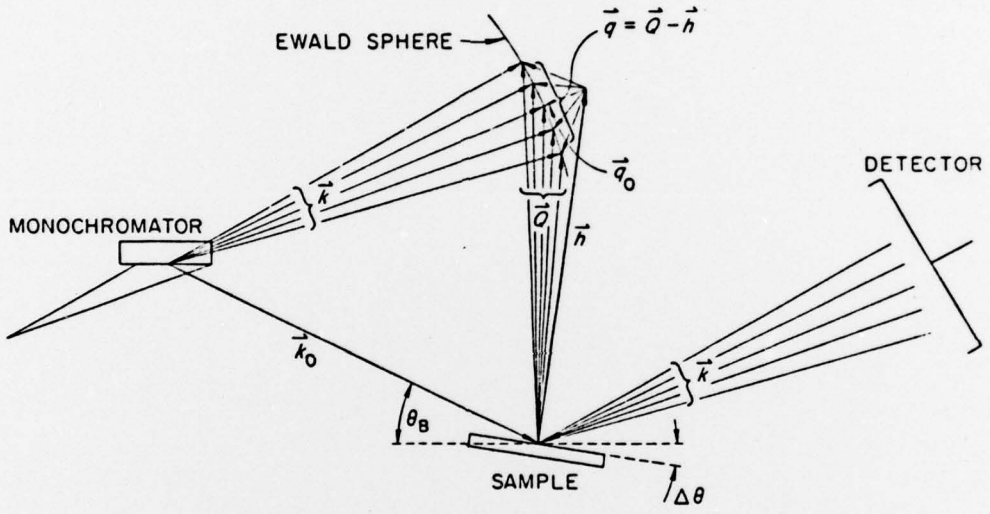

Figure 1. X-Ray Scattering Geometry for the Double-Crystal Measurements.

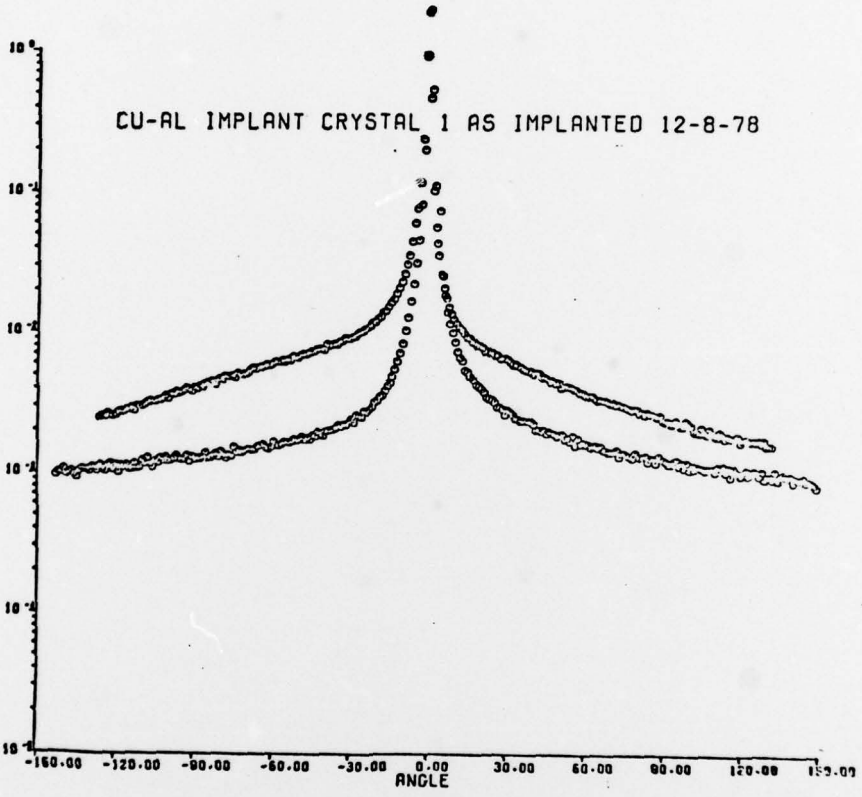

Figure 2. Scattering Rocking Curves (a) First Crystal Implanted and (b) Unimplanted.

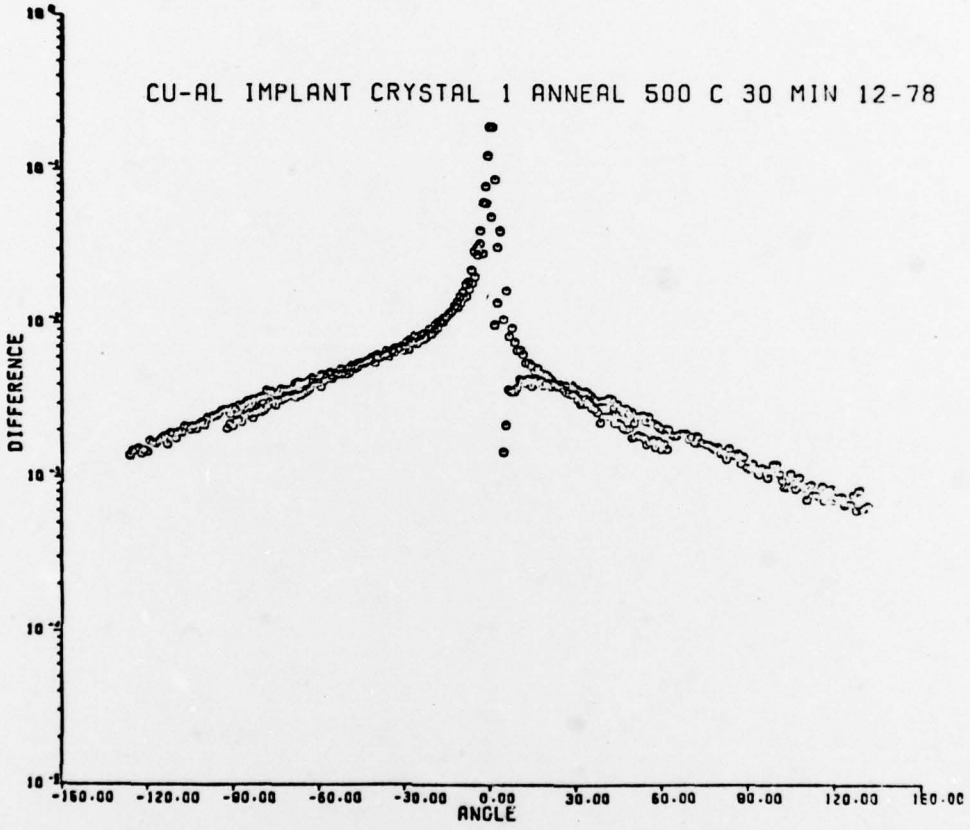

Figure 3. Implantation Scattering Intensity (a) First Crystal as Implanted and (b) Annealed at 500°C for 30 Minutes.

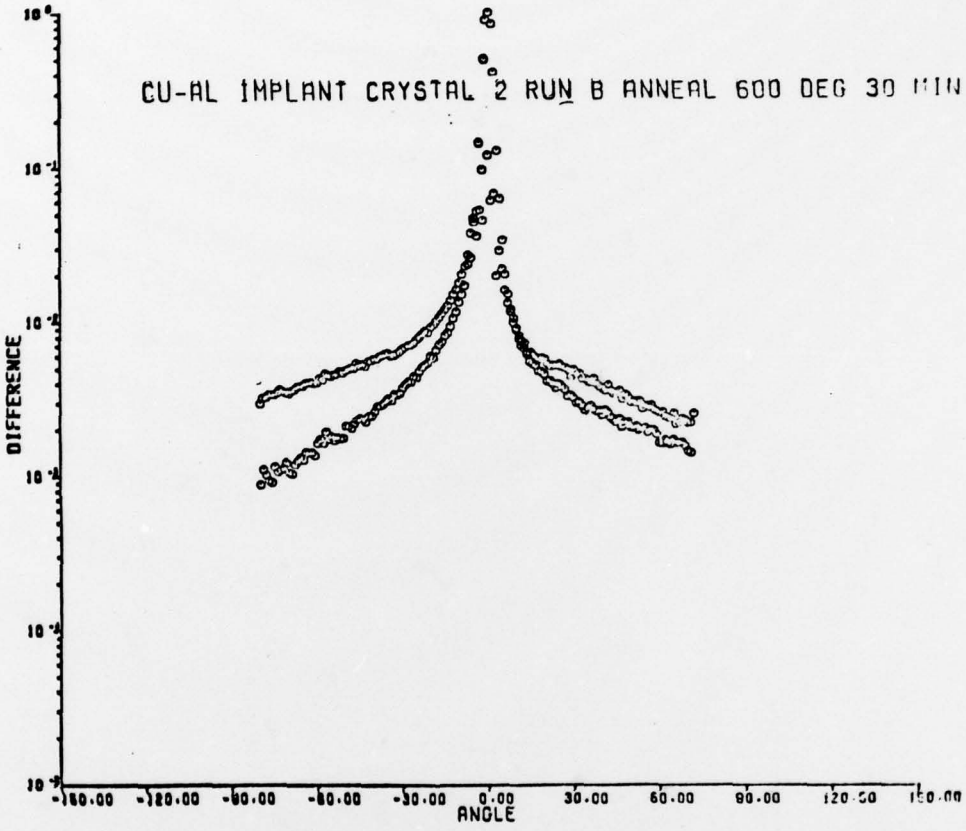

Figure 4. Implantation Scattering Intensity (a) Second Crystal As-Implanted and (b) Annealed at 600°C for 30 minutes.

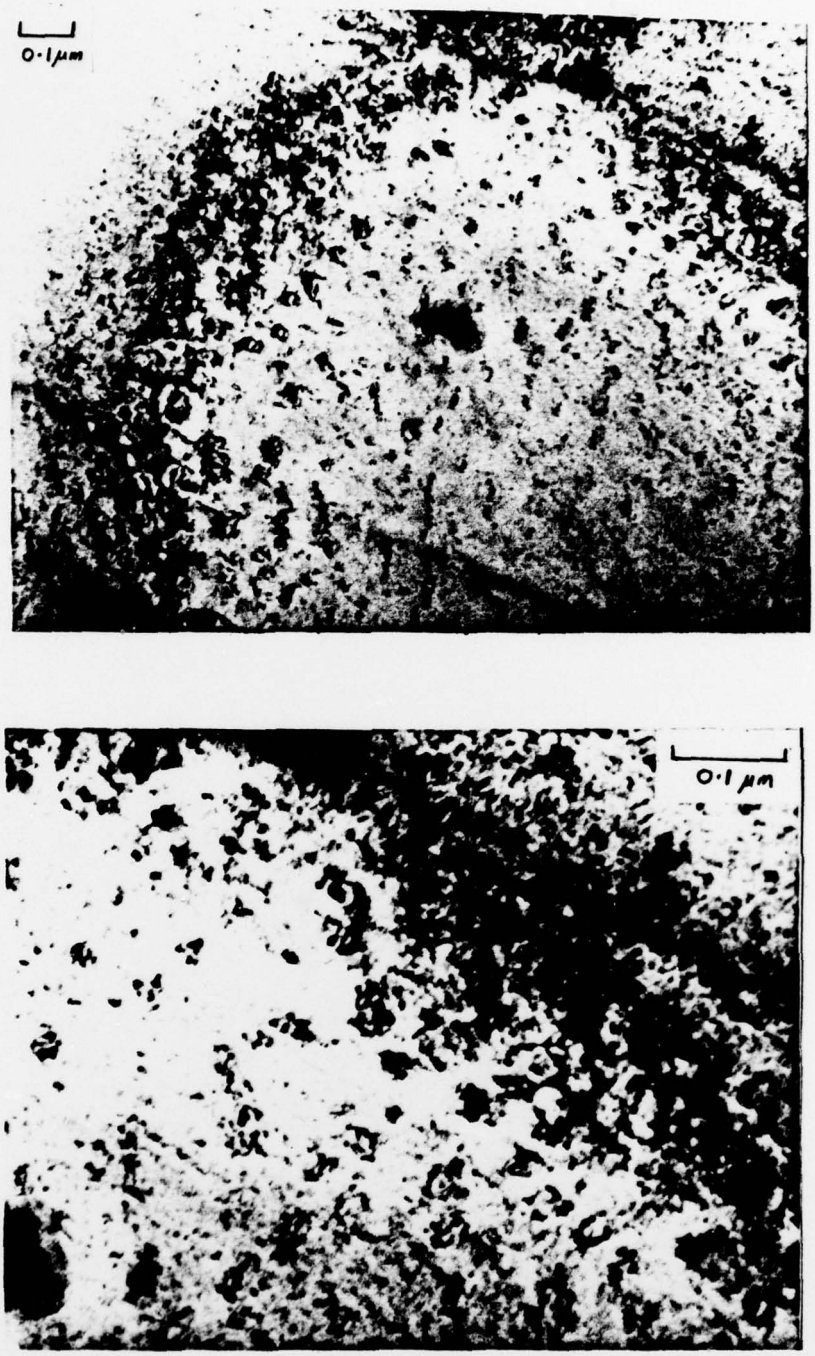

Figure 5. Transmission Electron Microscopy Micrographs Showing Effects of Argon Implantation ($2X10^{15}$ ions cm^{-2} at 100 kev). Many Large Loops Can Be Seen.

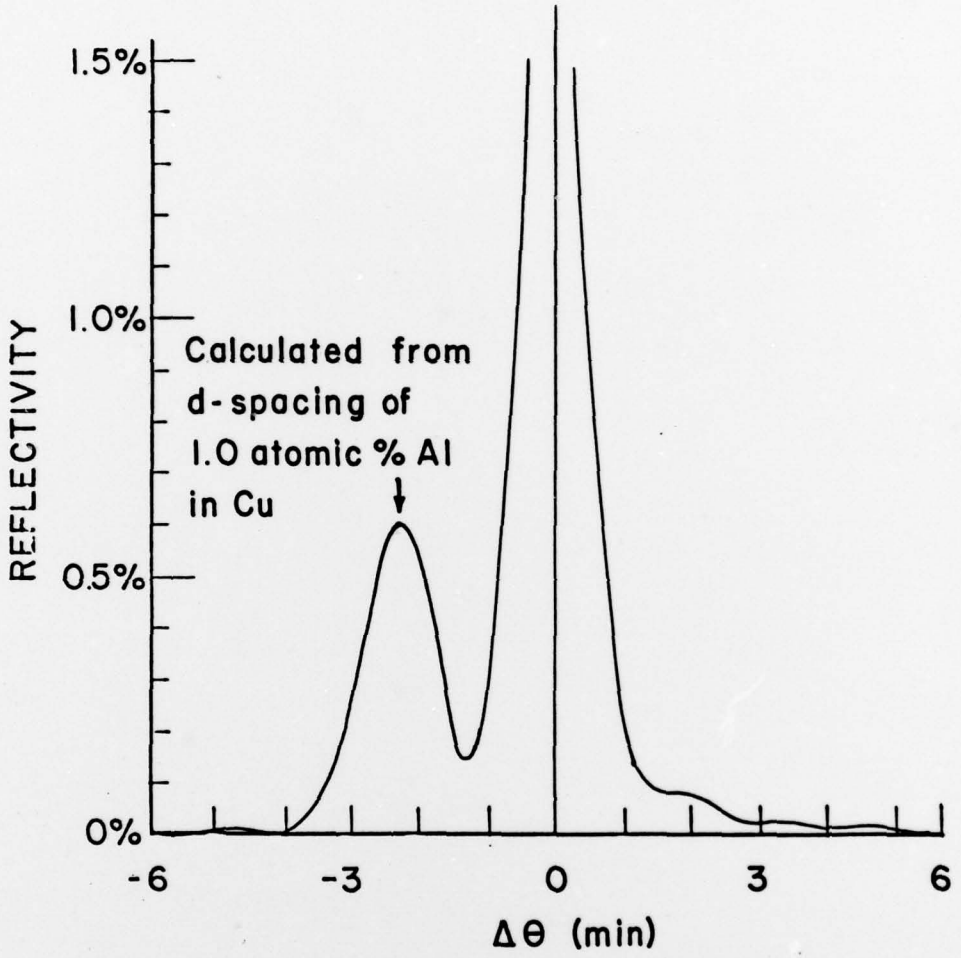

Figure 6. Calculated Reflectivity Versus Rocking Angle for a Copper Crystal Implanted With Aluminum to a Depth of 1300 Å at a Microscopic Concentration of 1 Atomic Percent.

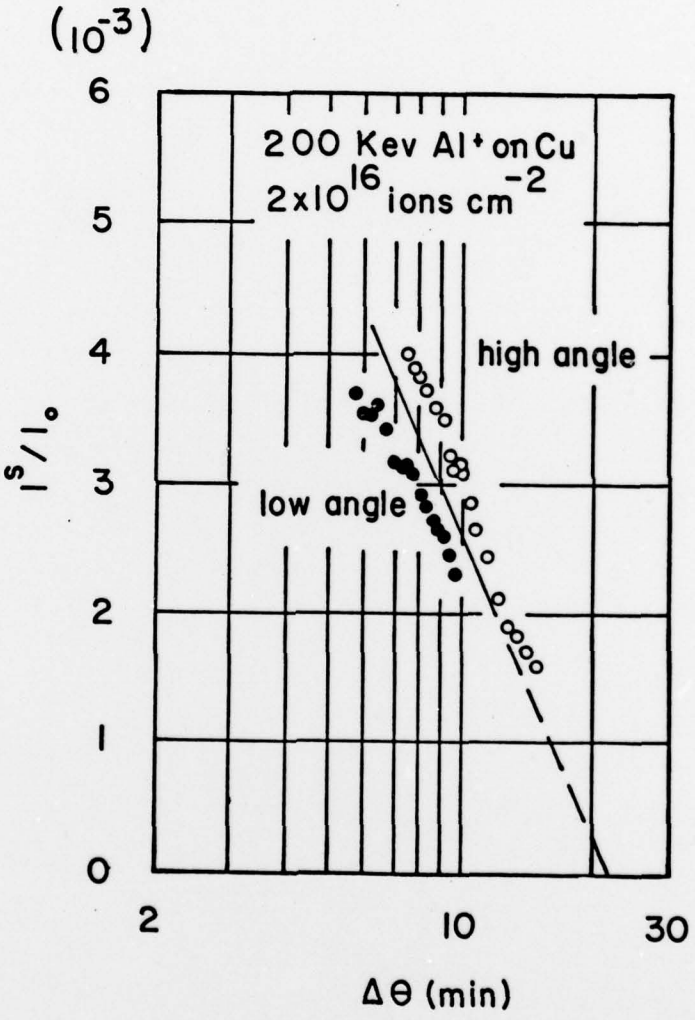

Figure 7. Diffuse Scattering From As-Implanted Sample Plotted as a Huang Scattering Curve I^s/I_o vs ln $\Delta\theta$.

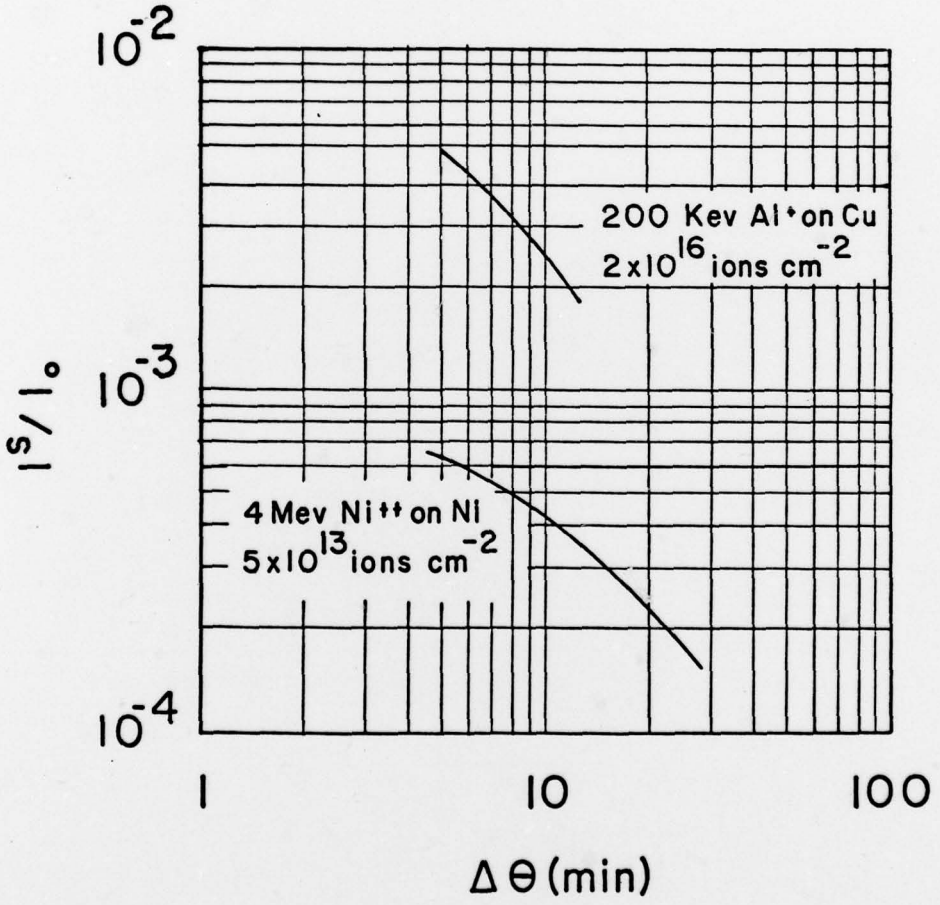

Figure 8. A Comparison of Huang Diffuse Scattering From Aluminum Implanted Copper (200 kev, $2X10^{16}$ ions cm^{-2}) and Nickel Implanted Nickel (4 Mev, $5X10^{13}$ ions cm^{-2}).